TASK QUARTERLY 11 No 4, 365–382

THE POLLUTANT TRANSPORT EQUATION FOR A STEADY, GRADUALLY VARIED FLOW IN AN OPEN CHANNEL NETWORK: A SOLUTION OF HIGH ACCURACY

ROMUALD SZYMKIEWICZ

Faculty of Civil and Environmental Engineering,
Gdansk University of Technology,
Narutowicza 11/12, 80-952 Gdansk, Poland
rszym@pg.gda.pl

(Received 15 July 2007)

Abstract: The paper is concerned with solving the transport pollutant problem for a steady, gradually varied flow in an open channel network. The 1D advective-diffusive transport equation is solved using the splitting technique. An analytical solution of the linear advective-diffusive equation in the form of an impulse response function is used to solve the advection-diffusion part of the governing equation. This approach, previously applied in solutions of the advection-diffusion equation for a single channel, is extended to a channel network. Numerical calculations are only required to compute the integral of convolution. The finite difference method is used to solve the second part of the governing equation, containing the source term. The applied approach has considerable advantages, especially appreciable in the case of advection-dominated transport with large gradients of concentration, since it generates no numerical dissipation or dispersion.

The flow parameters are obtained via solution of the steady, gradually varied flow equation. In the final non-linear system of algebraic equations obtained through approximation of the ordinary differential equation, the depths at each cross-section of channels and the discharge at each branch of the network are considered as unknowns. The system is solved using the modified Picard iteration, which ensures convergence of the iterative process for a steady, gradually varied flow solved for both looped and tree-type open channel networks.

Keywords: steady gradually varied flow, advection-diffusion equation, splitting technique, integral of convolution

1. Introduction

A passive substance dissolved in water is transported in an open channel according to the following 1D equation:

$$\frac{\partial(Af)}{\partial t}+\frac{\partial(Qf)}{\partial x}-\frac{\partial}{\partial x}\left(DA\frac{\partial f}{\partial x}\right)-\varphi=0, \tag{1}$$

where t is time, x – a spatial coordinate, f – concentration, D – the coefficient of longitudinal diffusion, A – cross-sectional area, Q – discharge, and φ – a source term.

The main problem of numerical solutions of Equation (1) with dominating advection is ensuring adequate accuracy of the solution. The truncation error introduced with the approximation of derivatives in a transport equation is well known to change the amplitudes and phase celerities of the waves representing the equation's exact solution. As the finite difference method uses the function's Taylor series expansion, truncation error will always occur and, consequently, numerical schemes will always generate dissipation or dispersion errors. This is why strong smoothing or unphysical oscillations of numerical solutions are often observed. Many algorithms, using either finite difference or finite element methods, have been proposed in recent years to improve the accuracy of numerical solutions. The nature of the advective-diffusive transport equation and the problems connected with its numerical solution have been discussed in detail by Fletcher [1], Gresho and Sani [2], and others.

The flow parameters present in Equation (1) can be obtained by solving the flow equation. It has been assumed that a steady, gradually varied flow (SGVF) takes place in the considered open channel network. The SGVF's governing equations can be obtained by simplifying the well-known system of de Saint-Venant equations [3]. The derivatives over time disappear for a steady flow and the lateral inflow is assumed to be negligible. Consequently, the continuity equation is reduced to the following form:

$$\frac{dQ}{dx} = 0, \tag{2}$$

whereas the momentum equation becomes as follows:

$$\frac{d}{dx}\left(\frac{\alpha Q^2}{A}\right) + gA\frac{dH}{dx} = -gAS, \tag{3}$$

with

$$S = \frac{n^2|Q|Q}{R^{4/3}A^2}, \tag{4}$$

where H is water surface elevation, S – slope friction, n – the Manning coefficient, g – gravitational acceleration, α – the Coriolis coefficient. $R = A/p$ is hydraulic radius and p – the wetted perimeter.

Equation (3) can be further rearranged as follows:

$$\frac{d}{dx}\left(H + \frac{\alpha Q^2}{2gA^2}\right) = -S. \tag{5}$$

The expression in brackets represents the total flow energy above the assumed value.

Equation (5) describes a flow profile, $H(x)$, along the channels. The following problem is formulated to calculate this function for a channel network: the $H(x)$ function should satisfy the governing equation and the imposed conditions at the upstream and downstream ends of the channel network defined by water levels. Moreover, discharges, Q, are unknown in all branches. The problem formulated in this manner can be considered as a boundary problem for the system of ordinary differential Equations (2) and (3). Unfortunately, while the shooting method, in which an initial value problem for an ordinary differential equation is solved repeatedly, can be used to solve the classical two-points boundary problem [4–6] it is useless for channel networks and thus the solution becomes more complicated.

Naindu, Murty Bhallamudi and Narasimhan [7] have proposed solving the SGVF equation for a channel network by decomposing the network into smaller units, solving

them using the IV order Runge-Kutta method and connecting the solutions to obtain the final solution for the whole network using the shooting method. However, the proposed algorithm holds for tree-type networks only.

A more general approach, suitable for any tree-type or looped network, is to solve the energy Equation (5) directly. To this order, the equation is simultaneously approximated for the entire network. Since natural rivers have variable cross-sections, only the Adams-Moulton method of lowest order (the trapezoidal rule) can be applied in this instance. It is absolutely stable and uses cross-sectional parameters at grid points only. In this approach, only depths at each grid point and discharge over an entire branch are considered as unknowns. This process produces a large system of non-linear algebraic equations, which should be solved by an iterative method. Since the Newton method often suffers from slow convergence or even lack of convergence, the modified Picard iteration is applied, which ensures a convergent solution of the SGVF equation for an open channel network of any type and any boundary conditions.

In the steady flow case, the 1D linear advective-diffusive equation of pollutant transport can be solved without approximation of derivatives. In this approach, the exact solution of the advective-diffusive equation, with constant coefficients obtained for the upstream boundary condition in the form of a Dirac delta function, is used. Therefore, instead of a system of algebraic equations given by the finite difference or element method, an integral of convolution must be calculated numerically using the quadrature method only. The convolution approach, successful for SGVF in a single channel [8], is developed below for an open channel network.

2. Solution of the SGVF equation for an open channel network

The finite difference method is applied to solve the boundary problem for the ordinary differential equations. A channel of length $\langle 0, L\rangle$ is divided by N nodes into $N-1$ intervals Δx_i. Equation (5) is approximated in the middle of each interval $x_i + \Delta x_i/2$ by centred difference, coincident with the implicit trapezoidal rule, a method with two important advantages: it is absolutely stable and ensures approximation of the second order of accuracy [4]. Its application to solve Equation (5) with the friction slope, S, defined by Equation (4) yields:

$$\left(H_{i+1} + \frac{\alpha Q^2}{2gA_{i+1}^2}\right) - \left(H_i + \frac{\alpha Q^2}{2gA_i^2}\right) + \frac{\Delta x_i}{2}\left(\frac{n^2 Q|Q|}{R_i^{4/3}A_i^2} + \frac{n^2 Q|Q|}{R_{i+1}^{4/3}A_{i+1}^2}\right) = 0, \qquad (6)$$

where i is the index of a cross-section and Δx_i – the length of interval of number i.

Similar equations can be written for each interval $\Delta x_i (i = 1,2,\ldots,N-1)$. We thus obtain a system of $N-1$ algebraic equations with $N+1$ unknowns. There are N water levels H_i at the nodes and flow discharge Q in the channel. When flow in a single channel is considered, this system needs to be completed with two additional equations obtained from the imposed boundary conditions. Assuming subcritical flow in the channel [9], the following conditions should be imposed at its ends:

$$H_1 = H_u, \qquad H_N = H_d, \qquad (7)$$

where H_u and H_d are the water levels imposed at, respectively, the upstream and downstream end of the channel.

The final system of equations can be presented in matrix form as follows:

$$\boldsymbol{A}\boldsymbol{X} = \boldsymbol{B}, \tag{8}$$

where $\boldsymbol{A}$ – matrix of coefficients, $\boldsymbol{B} = (H_u, 0, \ldots, 0, H_d, 0)^T$ – vector of the right hand side, $\boldsymbol{X} = (H_1, H_2, \ldots, H_{N-1}, H_N, Q)^T$ – vector of unknowns, T – transposition symbol.

Matrix $\boldsymbol{A}$ of dimensions $(N+1)\times(N+1)$ is very sparse (see Figure 1), with its non-zero elements defined as follows:

$$a_{1,1} = 1, \qquad a_{1,N+1} = \frac{\alpha Q}{2gA_1^2}, \tag{9a}$$

$$a_{i,i} = 1, \qquad a_{i,i-1} = -1 \qquad \text{for } i = 2,3,\ldots,N-1, \tag{9b}$$

$$a_{i,N+1} = -\frac{\alpha Q}{2gA_{i-1}^2} + \frac{\alpha Q}{2gA_i^2} + \frac{\Delta x_{i-1}}{2}\left(\frac{n^2|Q|}{R_{i-1}^{4/3}A_{i-1}^2} + \frac{n^2|Q|}{R_i^{4/3}A_i^2}\right) \qquad \text{for } i = 2,3,\ldots,N-1, \tag{9c}$$

$$a_{N,N} = 1, \qquad a_{N,N+1} = \frac{\alpha Q}{2gA_N^2}, \tag{9d}$$

$$a_{N+1,N-1} = -1, \qquad a_{N+1,N} = 1, \tag{9e}$$

$$a_{N+1,N+1} = -\frac{\alpha Q}{2gA_{N-1}^2} + \frac{\alpha Q}{2gA_N^2} + \frac{\Delta x_{N-1}}{2}\left(\frac{n^2|Q|}{R_{N-1}^{4/3}A_{N-1}^2} + \frac{n^2|Q|}{R_N^{4/3}A_N^2}\right). \tag{9f}$$

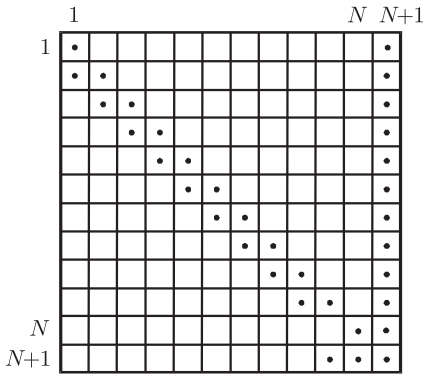

Figure 1. Structure of matrix $\boldsymbol{A}$; dots represent non-zero elements

When flow in a channel network is considered, subcritical flow is assumed in all branches. A set of equations in the form of Equation (8) can be written for each channel. Additionally, the following continuity equation is applicable for the junction of channels I, J, K formed by nodes i, j, k (see Figure 2):

$$Q_K = Q_I + Q_J, \tag{10}$$

as well as the energy equations:

$$H_i + \frac{\alpha Q_I^2}{2gA_i^2} = H_j + \frac{\alpha Q_J^2}{2gA_j^2} = H_k + \frac{\alpha Q_K^2}{2gA_k^2}. \tag{11}$$

Losses have been neglected in the above equations; sometimes the velocity heads can be also neglected, being relatively small.

Three additional equations in the form of Equations (10) and (11) should be written for each junction of the considered channel network, enabling us to close the global system of equations for the entire network. The matrix of this system contains submatrices describing each channel in the form presented in Equation (8), connected by the junction equations. The final matrix may be quite large, but it is always banded and very sparse.

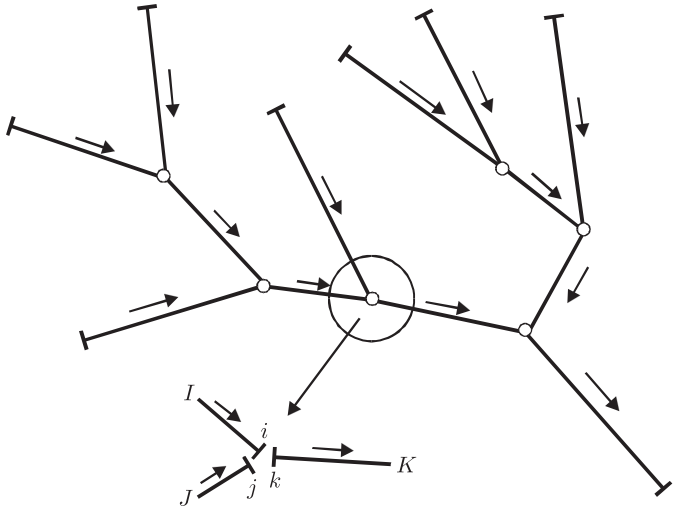

Figure 2. Open channel network; arrows indicate positive flow direction

The Picard iterative scheme applied for Equation (8) yields:

$$\boldsymbol{A}(\boldsymbol{X}^{(l)})\boldsymbol{X}^{(l+1)} = \boldsymbol{B}, \tag{12}$$

where l is the iteration index. Unfortunately, regardless of the first approximation of discharge Q, it is impossible to obtain a solution of the considered system. The computation shows that water levels tend to the expected values relatively quickly, whereas discharge $Q^{(l)}$ oscillates during subsequent iterations with a constant amplitude. In order to suppress these oscillations, Szymkiewicz and Szymkiewicz [10] have proposed the following improvement of the Picard method:

$$\boldsymbol{A}^* \boldsymbol{X}^{(l+1)} = \boldsymbol{B}, \tag{13}$$

where

$$\boldsymbol{A}^* = \boldsymbol{A}\left(\frac{\boldsymbol{X}^{(l)} + \boldsymbol{X}^{(l-1)}}{2}\right) \tag{14}$$

is a modified matrix of coefficients. This means that, in order to calculate vector $\boldsymbol{X}$ in iteration $l+1$, matrix $\boldsymbol{A}$ is calculated using the average value of $\boldsymbol{X}$ from two preceding iterations. For $l=1$, $\boldsymbol{A}^* = \boldsymbol{A}(\boldsymbol{X}^{(0)})$ is recommended.

Having assumed the first estimation of the unknown vector $\boldsymbol{X}^{(0)}$, the iterative process is continued until two succeeding solutions satisfy the following convergence criteria:

$$\left|X_i^{(l+1)} - X_i^{(l)}\right| \le \varepsilon_H \quad \text{for } i=1,\ldots,N \quad \text{and} \quad \left|X_{N+1}^{(l+1)} - X_{N+1}^{(l)}\right| \le \varepsilon_Q, \tag{15}$$

where ε_H and ε_Q respectively represent the specified tolerances for water level H_i and discharge Q.

Although an iterative method seems suitable for solving Equation (12), which is a system of linear algebraic equations with a very sparse matrix of coefficients, attempts to solve it with the Gauss-Seidel or SOR methods have failed. Finally, Equation (12) has been solved by the Gauss elimination method in its frontal version, which uses non-zero elements of matrix $\boldsymbol{A}$ only.

3. Solution of the transport equation by splitting

After differentiating the first two terms of Equation (1) and taking into account the continuity equation for open channel flow without lateral inflow [9], we obtain:

$$\frac{\partial f}{\partial t}+U\frac{\partial f}{\partial x}-\frac{1}{A}\frac{\partial}{\partial x}\left(DA\frac{\partial f}{\partial x}\right)-\varphi=0, \tag{16}$$

where $U=Q/A$ – cross sectional average velocity, φ – source term.

An approach based on the splitting technique is applied to solve the above equation. Equation (16) can be rewritten in the following form:

$$\frac{\partial f}{\partial t}+F^{(1)}+F^{(2)}=0, \tag{17}$$

where

$$F^{(1)}=U\frac{\partial f}{\partial x}-\frac{1}{A}\frac{\partial}{\partial x}\left(DA\frac{\partial f}{\partial x}\right) \quad \text{and} \quad F^{(2)}=-\varphi. \tag{18}$$

Consequently, the solution of Equation (17) can be split in two stages for every time step Δt [8]. In the first stage, advective-diffusive transport without the source term is solved:

$$\frac{\partial f^{(1)}}{\partial t}+U\frac{\partial f^{(1)}}{\partial x}-\frac{1}{A}\frac{\partial}{\partial x}\left(DA\frac{\partial f^{(1)}}{\partial x}\right)=0, \tag{19}$$

with the initial condition of $f^{(1)}(t)=f(t)$. In the second stage, the equation containing only the source term:

$$\frac{\partial f^{(2)}}{\partial t}=\varphi, \tag{20}$$

is solved with the initial condition being the solution of Equation (19), $f^{(2)}(t)=f^{(1)}(t+\Delta t)$. Finally, we obtain $f(t+\Delta t)=f^{(2)}(t+\Delta t)$. Equations (19) and (20) are solved respectively using the convolution approach and the finite difference method.

Let us consider Equation (19) in which the superscript has been omitted for the sake of simplicity:

$$\frac{\partial f}{\partial t}+U\frac{\partial f}{\partial x}-\frac{1}{A}\frac{\partial}{\partial x}\left(DA\frac{\partial f}{\partial x}\right)=0, \tag{21}$$

where $U=U(x)$ is the average cross-sectional velocity.

For constant coefficients ($U=\text{const}$, $D=\text{const}$, $A=\text{const}$) and the initial and boundary conditions $f(x,t=0)=0$, $f(x=0,t)=\delta(t)$ and $f(x=\infty,t)=0$ for $t\geq 0$, Equation (21) has an exact solution [11]:

$$f(x,t)=\frac{1}{(4\pi D)^{1/2}}\frac{x}{t^{3/2}}\exp\left(-\frac{(Ut-x)^2}{4Dt}\right). \tag{22}$$

The $f(x,t)$ function is the output at any cross-section located at x when the Dirac delta function, $\delta(t)$ [12], is imposed at $x=0$ as input. Therefore, $f(x,t)$ can

be considered as an impulse response of the system in the form of a channel section of length x. Equation (22) holds for $t>0$ and $x>0$. This function is never negative ($f(x,t)\geq 0$ for $t>0$), has a single peak and its integral over time is equal to unity. Its location along the time axis is determined by U and x, whereas its shape is determined by the coefficient of diffusion, D. For decreasing values of D, the function becomes ever sharper and more symmetrical. For $D\to 0$, the $f(x,t)$ function tends to the Dirac delta function, $\delta(t)$. In hydrology, Equation (22) is known as an instantaneous unit hydrograph (IUH) for a linear diffusive wave [11].

Knowing the impulse response function and using the convolution, we can calculate the output for any input. The convolution approach to solving the advection-diffusion equation holds for steady uniform flows. However, in natural streams a steady flow is spatially varied, *i.e.* its velocity and cross-sectional area vary along the x axis. Fortunately, the convolution approach can also be adapted for steady, gradually varied flows [8].

After differentiation of the diffusive term, Equation (21) assumes the following form:

$$\frac{\partial f}{\partial t}+\left(U-\frac{\partial D}{\partial x}-\frac{D}{A}\frac{\partial A}{\partial x}\right)\frac{\partial f}{\partial x}-D\frac{\partial^2 f}{\partial x^2}=0. \tag{23}$$

In this equation, advective velocity and diffusivity vary in space. The $U(x)$ and $A(x)$ functions are given by solutions of Equations (2) and (3). In order to solve Equation (23) using convolution, we can freeze velocity and diffusivity locally as follows. A channel of length L is divided into M intervals of length Δx_i as in the finite difference or finite element method (see Figure 3a). Each channel section is considered as a dynamic system in which advective velocity and the coefficient of diffusion are assumed to be constant. Now, we introduce two new variables defined as follows:

$$u_i=\frac{1}{2}\left[\left(U-\frac{\partial D}{\partial x}-\frac{D}{A}\frac{\partial A}{\partial x}\right)_{i-1}+\left(U-\frac{\partial D}{\partial x}-\frac{D}{A}\frac{\partial A}{\partial x}\right)_{i}\right]\approx$$
$$\approx\frac{1}{2}\left[\left(U_{i-1}-\frac{D_i-D_{i-1}}{\Delta x_i}-\frac{D_{i-1}}{A_{i-1}}\frac{A_i-A_{i-1}}{\Delta x_i}\right)+\left(U_i-\frac{D_i-D_{i-1}}{\Delta x_i}-\frac{D_i}{A_i}\frac{A_i-A_{i-1}}{\Delta x_i}\right)\right], \tag{24}$$

$$d_i=\frac{1}{2}(D_{i-1}+D_i), \tag{25}$$

where u_i is the modified average advective velocity between node $i-1$ and node i and d_i – the average coefficient of diffusion between node $i-1$ and node i.

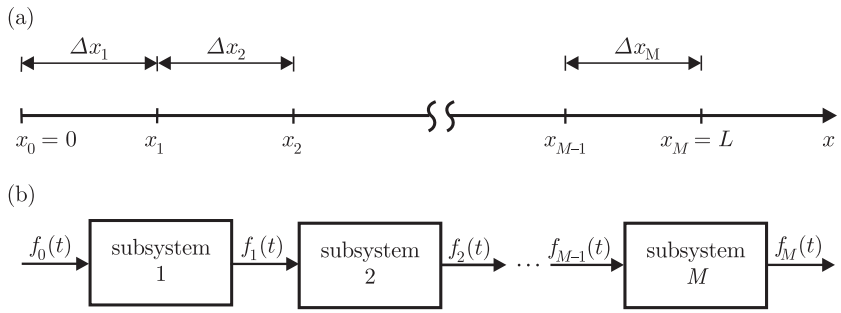

Figure 3. A scheme of a channel: (a) divided into intervals of length Δx_i and (b) represented by M subsystems [8]

A river section of length Δx_i, bounded by cross-sections $x = x_{i-1}$ and $x = x_i$, is considered as a dynamic, linear and time-invariant system. Therefore, accordingly to Equation (22), its response function is as follows:

$$h_i(t) = \frac{1}{(4\pi d_i)^{1/2}} \frac{\Delta x_i}{t^{3/2}} \exp\left(-\frac{(u_i t - \Delta x_i)^2}{4 d_i t}\right). \tag{26}$$

The $f_i(t)$ function is calculated for nodes located along the channel axis ($i = 1,2,3,\ldots$, see Figure 3b) using the following convolution integral:

$$f_i(t) = \int_0^{m_i} h_i(\tau) f_{i-1}(t-\tau) d\tau, \tag{27}$$

where m_i is the memory of system i.

This means that an output at time t is determined by an input taken from time interval $\langle t - m_i, t\rangle$, as the $h(t)$ function insignificantly differs from zero for $t \geq m_i$. Let us remember that a channel of length L, which has been divided into sections of length Δx_i, is considered as a series of M subsystems, where the output from one section is the input to the next (see Figure 3b). Integration can be performed with the trapezoidal rule and time step equal to $\Delta\tau$. The value of $f_i(t-\tau)$ is calculated using linear interpolation. Application of Equation (27) will be successful provided that the balance of mass is maintained [8].

At the second stage of solving the transport equation, Equation (20) must be solved, using the solution of previously solved Equation (21). The domain of solution ($0 \leq x \leq L$ and $t \geq 0$) is covered by grid points as in the finite difference method. The mesh resulting of dimensions $\Delta x \cdot \Delta t$ is presented in Figure 4.

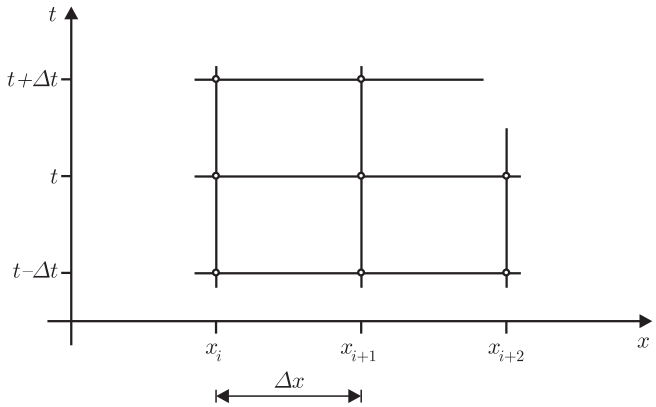

Figure 4. The grid points applied to solve Equation (20)

It should be remembered that a constant flow velocity U has been assumed between cross-sections x_i and x_{i+1}. Let us also assume that concentration f is known at all grid points until time level t and at point x_i at time level $t + \Delta t$. The aim is to calculate concentration f at point $(x_{i+1}, t + \Delta t)$. As Equation (21) has been solved during the first stage using the convolution approach:

$$f_{i+1}^{(1)}(t + \Delta t) = \int_0^{m_i} h_i(\tau) f_i(t - \tau) d\tau, \tag{28}$$

$f^{(1)}(t+\Delta t)$ is known. In the second stage, the final concentration at node $(x_{i+1}, t+\Delta t)$ is obtained by solving Equation (20):

$$\frac{\partial f^{(2)}}{\partial t} = \varphi, \tag{29}$$

with the initial condition $f^{(2)}(t) = f^{(1)}(t+\Delta t)$.

In order to cover the distance between cross-sections x_i and x_{i+1}, a particle of dissolved matter requires time equal to:

$$\Delta T = \frac{\Delta x}{U_i}. \tag{30}$$

During this time, the pollutant decays and the effect of this process must be taken into account when integrating Equation (29) in the second step of the solution process. Solving Equation (29) by the trapezoidal rule yields:

$$f_{i+1}^{(2)}(t+\Delta t) = f_{i+1}^{(1)}(t+\Delta t) + \frac{\Delta T}{2}\left(\varphi_{i+1}^{(1)}(t+\Delta t) + \varphi_{i+1}^{(2)}(t+\Delta t)\right), \tag{31}$$

where: i is a cross-section's index, ΔT – the time of a particle travelling from cross-section i to cross-section $i+1$ and Δt – mesh dimensions in the t direction.

This method is absolutely stable and ensures the second order of accuracy with regard to t [4]. If the source term depends on concentration f, Equation (31) will become non-linear and, consequently, an iterative method will have to be applied for its solution.

In order to solve the problem of pollutant transport in an open channel network, additional relations resulting from the mass conservation principle must be introduced for each junction or bifurcation of the channels. The following equation holds for a junction of two channels, as presented in Figure 5a:

$$f_k = \frac{f_i Q_i + f_j Q_j}{Q_i + Q_j}, \tag{32}$$

whereas the following relations are valid for a channel bifurcation, as presented in Figure 5b:

$$f_k = f_i \quad \text{and} \quad f_k = f_j. \tag{33}$$

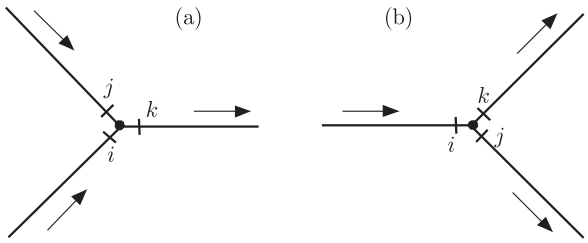

Figure 5. Junction (left) and bifurcation (right) of the channels; arrows indicate the positive flow direction

Equations (32) and (33) allow us to solve the advective-diffusive transport equation for the entire network.

4. Numerical experiments

4.1. Test 1

SGVF is considered in the looped channel network shown in Figure 6.

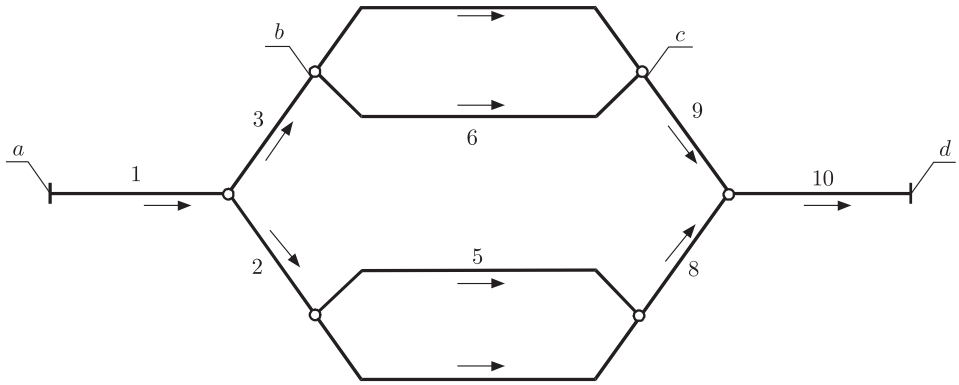

Figure 6. Looped channel network

It consists of 10 branches of trapezoidal cross-sections. Each channel is divided into sections of constant length. The network's characteristics are presented in Table 1.

Table 1. Channel characteristics for the network shown in Figure 6

Channel	Length [m]	Bed width [m]	Side slope	Bed slope	n	Δx [m]
1	500	5.0	1.5	0.0005	0.035	50
2	500	5.0	1.5	0.0005	0.035	50
3	500	5.0	1.5	0.0005	0.035	50
4	1000	5.0	1.5	0.0005	0.035	50
5	1000	5.0	1.5	0.0005	0.035	50
6	1000	5.0	1.5	0.0005	0.035	50
7	1000	5.0	1.5	0.0005	0.035	50
8	500	5.0	1.5	0.0005	0.035	50
9	500	5.0	1.5	0.0005	0.035	50
10	500	5.0	1.5	0.0005	0.035	50

The total number of nodes equals 159. Bed elevation is 10.000 m at the upstream end (point a) and 8.500 m at the downstream end (point d). The boundary conditions, specified in terms of water levels at the upstream and downstream ends of network, are as follows: $H_a = 11.750$ m, $H_d = 11.500$ m.

Numerical tests have demonstrated that the modified Picard method is capable of producing very good results. The proposed approach ensures a convergent solution regardless of the first estimation of discharge in the channels. For $Q_i^{(0)}$ $(i = 1,2,\ldots,10)$ equal to $15\,\mathrm{m}^3/\mathrm{s}$, a solution of tolerances $\varepsilon_H = 0.001$ m and $\varepsilon_Q = 0.001\,\mathrm{m}^3/\mathrm{s}$ was obtained after 16 iterations. The calculation results for the network shown in Figure 6 and characterized in Table 1 are presented in Table 2.

Table 2. Results for the network shown in Figure 6

Channel	Discharge [m^3/s]	Upstream water level [m]	Downstream water level [m]
1	9.706	11.750	11.575
2	4.853	11.575	11.544
3	4.853	11.575	11.544
4	2.427	11.544	11.536
5	2.427	11.544	11.536
6	2.427	11.544	11.536
7	2.427	11.544	11.536
8	4.853	11.536	11.526
9	4.853	11.536	11.526
10	9.706	11.526	11.500

Let us now apply the convolution approach to solving the advective-diffusive transport equation for a steady uniform flow in the considered channel network. The flow's velocity, $U(x)$, and cross-sectional areas, $A(x)$, are known since they were calculated previously using the SGVF equation. The initial concentration is assumed to equal zero along all of the network's branches. The following $f_a(t)$ function is imposed at the beginning of channel 1 (*i.e.* at point a, see Figure 6):

$$f_1(t) = \begin{cases} 0 & \text{for} \quad t < 0.5h \\ f_m & \text{for } 0.5h \le t \le 1.5h \\ 0 & \text{for} \quad t > 1.5h \end{cases} \tag{34}$$

This means that a rectangular distribution of concentration is assumed (Figure 7, point a), a highly challenging test for the numerical method of solution.

The $f(t)$ functions at points b, c and d were calculated for a diffusion coefficient equal to $D = 0.00005\,\mathrm{m^2 s^{-1}}$. As the source term was neglected, one could expect that the imposed rectangular distribution of concentration would be transformed insignificantly, since the accepted value of the diffusion coefficient was very low. The obtained solutions are presented in Figure 7. Indeed, only the corners are rounded off in the concentration distribution calculated at points b, c and d. Due to the considered network's structure (see Figure 6), the distributions of concentration in all branches are deformed by diffusivity only. One may as well as suppose that the error generated by the implicit trapezoidal method used to integrate convolution was very low. The calculations were carried out for $\Delta\tau = 0.1\,\mathrm{s}$ and $\Delta t = 100\,\mathrm{s}$.

The Peclet number [13]:

$$P_c = \frac{U\Delta x}{D}, \tag{35}$$

for the data accepted in the considered example was greater than 750 000, which involves absolute domination of advection in the transport process. Notably, no oscillations, typical for the finite difference and finite element methods, were observed in the calculated distributions.

Our next example deals with the application of the proposed method to solving the advection-diffusion transport in the same network with the same set of data but

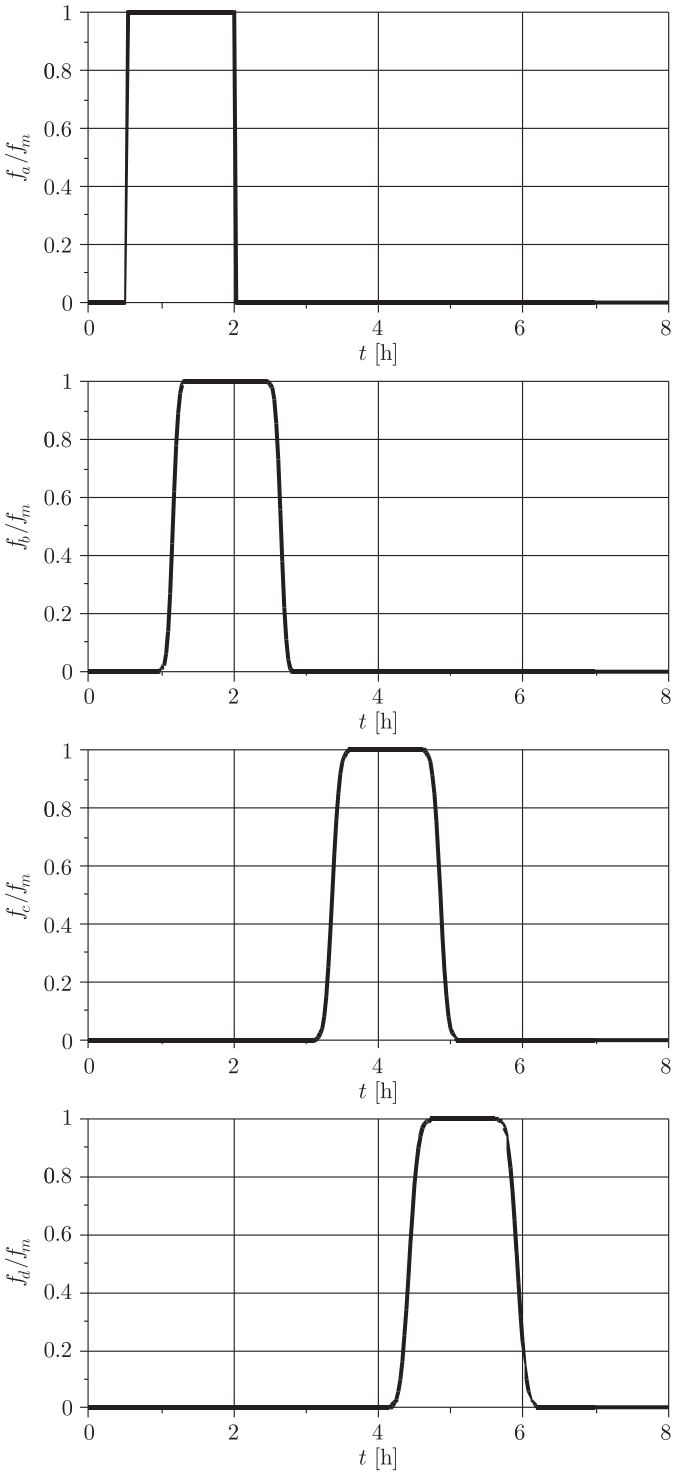

Figure 7. Advective-diffusive transport of initially rectangular distribution of concentration at selected points of the looped network with $D = 0.00005\,\mathrm{m}^2/\mathrm{s}$ and without the source term

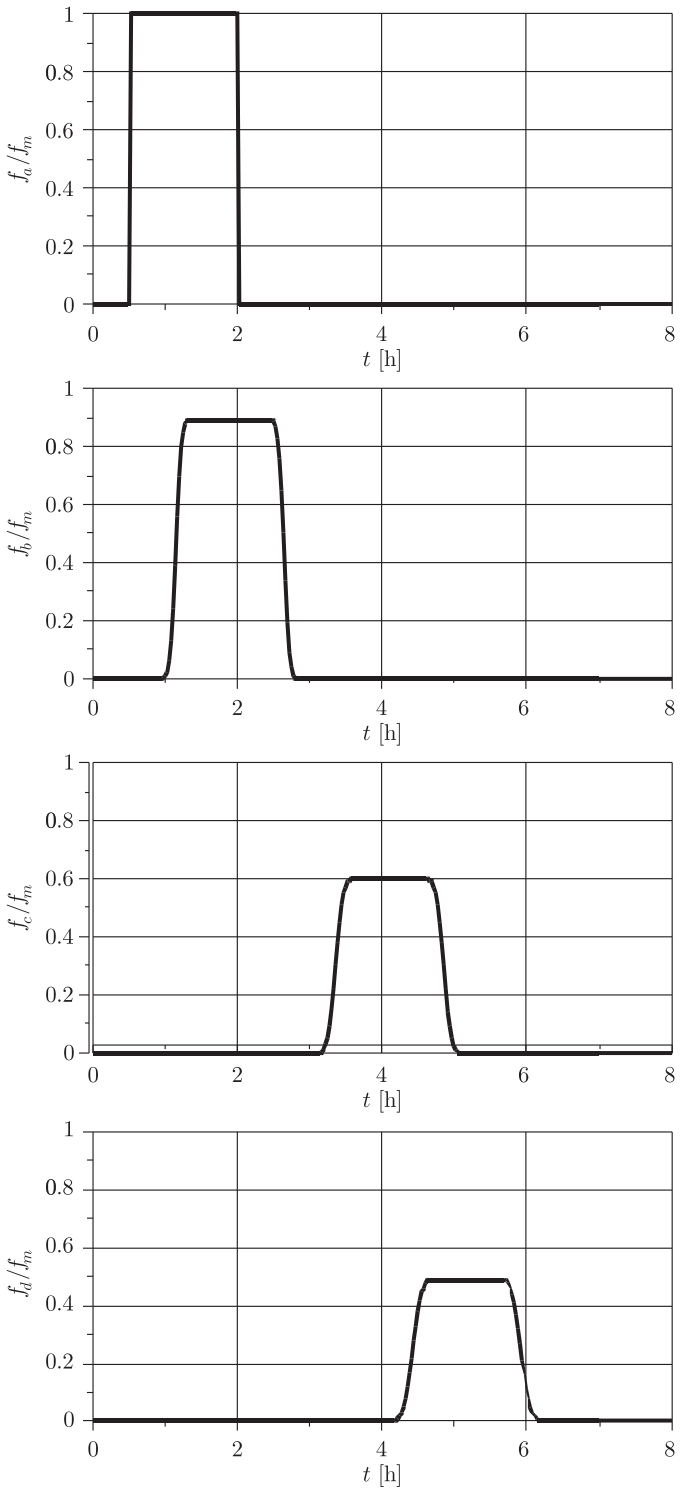

Figure 8. Advective-diffusive transport of initially rectangular distribution of concentration at selected points of the looped network with $D = 0.00005\,\mathrm{m}^2/\mathrm{s}$ and $\beta = 0.00005\,\mathrm{s}^{-1}$

with a source term describing the transported substance's decay. The simplest formula of the source term:

$$\varphi = \beta \cdot f, \tag{36}$$

where β is the constant of decay, was introduced into the transport equation. The distribution of concentration at selected points of the network shown in Figure 6 is presented in Figure 8. In this case, the travelling rectangular distribution of concentration is simultaneously subjected to two processes: smoothing due to diffusion and reduction due to the source term, in which $\beta = 0.00005\,\mathrm{s}^{-1}$. The obtained solution presented in Figure 8 appears to be close to the exact one, since in this case the source term has a linear form. Consequently, the splitting technique applied for the solution of the transport equation does not generate any additional error [14].

4.2. Test 2

This example deals with a tree-type channel network. The SGVF is considered in the channel network shown in Figure 9, consisting of 9 branches trapezoidal in cross-sections. Each channel is divided into intervals of constant length. The network's characteristics are presented in Table 3. The total number of nodes is 189 and bed elevations at the upstream ends are 5.000 m at point a, 4.850 m at point b, 4.800 m at point c, 4.750 m at point d and 4.750 m at point e. Bed elevation at the downstream end (point f) is 3.500 m. The boundary conditions are specified in terms of water levels at upstream (a, b, c, d, e) and downstream (f) ends of the network (see Table 4).

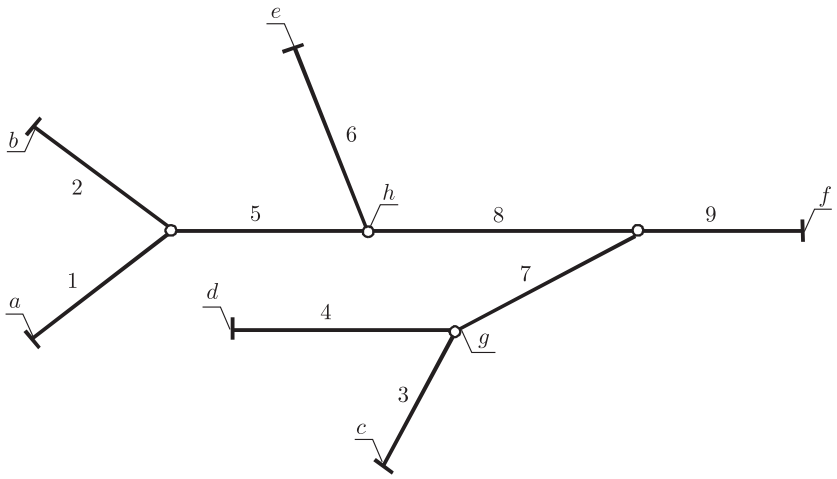

Figure 9. Tree-type channel network

For the initially assumed $Q_i^{(0)}$ $(i = 1,2,\ldots,9)$ equal to $5\,\mathrm{m}^3/\mathrm{s}$, a solution with tolerances $\varepsilon_H = 0.001\,\mathrm{m}$ and $\varepsilon_Q = 0.001\ \mathrm{m}^3/\mathrm{s}$ was obtained after 15 iterations. The results are given in Table 4.

As previously, the initial concentration of pollutant at $t = 0$ was assumed to be nil along all the network branches. Boundary conditions were imposed at the upstream ends of all pending branches. The imposed $f_a(t)$ and $f_c(t)$ functions assume the form of Equation (34) at points a and c, whereas at points b, d and e the corresponding functions are $f_b(t) = 0$, $f_d(t) = 0$, $f_e(t) = 0$ for $t \geq 0$, which means that the pollutant

Table 3. Channel characteristics for the network shown in Figure 9

Channel	Length [m]	Bed width [m]	Side slope	Bed slope	n	Δx [m]
1	500.0	2.50	1.5	0.0004	0.025	25.0
2	500.0	2.50	1.5	0.0003	0.025	25.0
3	500.0	2.50	1.5	0.0006	0.025	25.0
4	500.0	2.50	1.5	0.0006	0.025	25.0
5	500.0	4.00	1.5	0.0007	0.025	25.0
6	500.0	2.50	1.5	0.0005	0.025	25.0
7	500.0	3.00	1.5	0.0010	0.025	25.0
8	1500.0	5.00	1.5	0.00033	0.025	75.0
9	500.0	6.50	1.5	0.0005	0.025	25.0

Table 4. Results for the network shown in Figure 9

Channel	Discharge [m^3/s]	Upstream water level [m]	Downstream water level [m]
1	2.842	6.250	6.151
2	2.354	6.220	6.154
3	2.649	6.050	5.980
4	2.649	6.050	5.980
5	5.196	6.141	6.030
6	0.629	6.050	6.045
7	5.298	5.962	5.865
8	5.825	6.031	5.869
9	11.122	5.851	5.750

loads introduced at points a and c have been successively dissolved at each junction through mixing with pure water. Consequently, the initial rectangular distribution is reduced in the next branches even though the source term is omitted in the governing equation. Moreover, the concentration distributions are transformed by the diffusion process only. The computation results obtained for $\Delta\tau = 0.125\text{s}$, $\Delta t = 100\text{s}$, $D = 0.00005\text{m}^2/\text{s}$ and $\beta = 0$ are presented in Figure 10.

Results obtained for the same network (shown in Figure 9) and the same data set but with a source term of $\beta = 0.00002\text{s}^{-1}$ are shown in Figure 11. In this case, the initial rectangular distributions of concentration are reduced not only through mixing at the channel junctions, but also by pollutant decay. The effect of decay can be observed by comparing the corresponding graphs at points g, h, and f of Figures 10 and 11.

5. Conclusions

The equation of steady, gradually varied flow was integrated by means of the implicit trapezoidal rule to determine flow profiles and discharges in an open channel network. This approach yields a non-linear system of algebraic equations. If the depths at each grid point and the discharge over the whole channel are

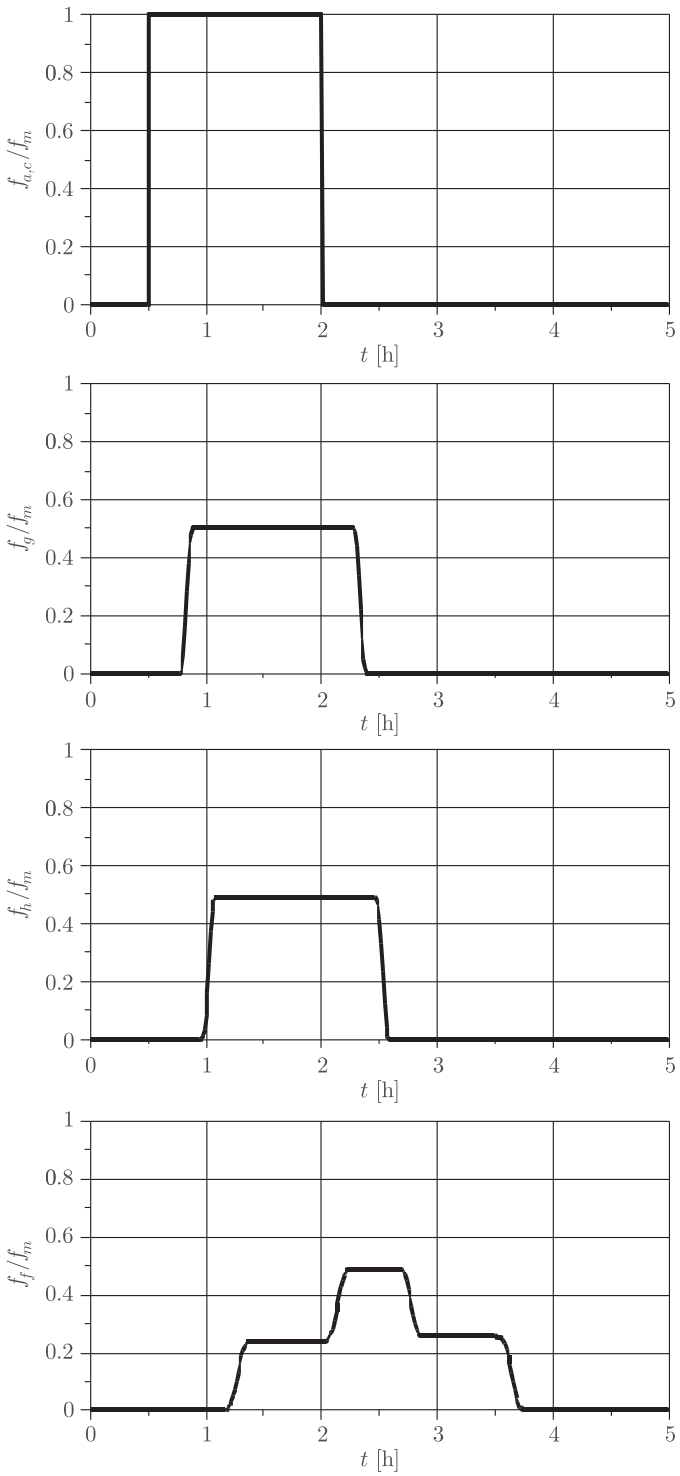

Figure 10. Advective-diffusive transport of initially rectangular distribution of concentration at selected points of the tree-type network with $D = 0.00005\,\mathrm{m}^2/\mathrm{s}$ and without the source term

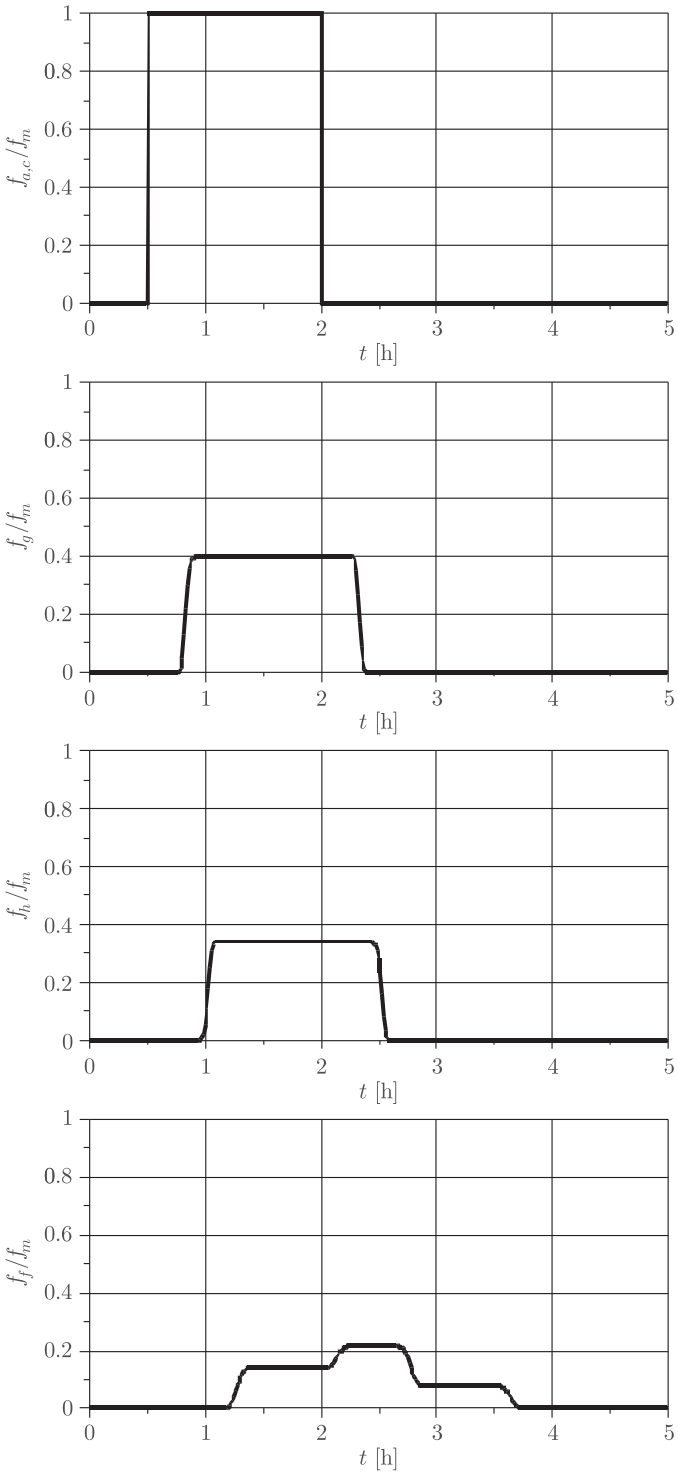

Figure 11. Advective-diffusive transport of initially rectangular distribution of concentration at selected points of the tree-type network with $D = 0.00005\,\mathrm{m}^2/\mathrm{s}$ and $\beta = 0.00005\,\mathrm{s}^{-1}$

considered as unknowns, the system cannot be solved using standard, *e.g.* Newton or Picard, methods due to the lack of convergence. Therefore, a modification of the Picard method was applied to ensure convergent iteration. Averages from two successive iterations were used to suppress saw-teeth. The Gauss elimination method adapted for sparse matrices of coefficients was used as a linear solver. The proposed improvement of the Picard method proved to be effective. The obtained calculation results have confirmed that the proposed approach can be applied for tree-type and looped networks when water levels or discharges at channel ends are imposed as boundary conditions. The iterative process is almost always convergent, for channel networks of any complexity.

The splitting technique was applied to solve the advective-diffusive transport equation with a source term. For a channel section of length Δx, considered as a linear and time-invariant system, the solution of the advection-diffusion transport equation may be presented in the form of a convolution integral. Considering a river section as a linear and time-invariant system, pollutant transport can be described by the differential advective-diffusive equation as well as the integral of convolution, the two approaches being equivalent. Therefore, instead of solving a differential equation with imposed initial and boundary conditions by the finite difference or element method, the integral of convolution may be calculated using the quadrature method only. Consequently, it will produce no numerical diffusion or dispersion. The calculation carried out for transport caused by steady, gradually varied flow has confirmed high accuracy of the obtained solution. The obtained results have shown the proposed approach to be helpful in solving advective-diffusive transport. The proposed algorithm has no limitations typical for numerical methods.

References

[1] Fletcher C A 1991 *Computational Techniques for Fluid Dynamics*, Vol. I, Springer Verlag, Berlin, Germany
[2] Gresho P M and Sani R L 1998 *Incompressible Flow and the Finite Element Method – Volume 1: Advection-Diffusion*, J. Wiley and Sons Ltd.
[3] French R H 1985 *Open Channel Hydraulics*, McGraw-Hill, New York
[4] Bjorck A and Dahlquist G 1974 *Numerical Methods*, Prentice-Hall, Englewood Cliffs, New Jork
[5] Stoer J and Bulirsch R 1980 *Introduction to Numerical Analysis*, Springer-Verlag, New York
[6] Press W H, Teukolsky S A, Veterling W T and Flannery B P 1992 *Numerical Recipes in C*, Cambridge University Press
[7] Naidu B J, Murty Bhallamudi S and Narasimhan S 1997 *J. Hydr. Engng* **123** (8) 700
[8] Szymkiewicz R and Weinerowska K 2005 *Far East J. Appl. Math.* **19** (24) 213
[9] Chow V T 1959 *Open Channel Hydraulics*, Mc Graw-Hill, New York
[10] Szymkiewicz R and Szymkiewicz A 2004 *Commun. Numer. Meth. Engng* **20** (4) 299
[11] Eagleson P S 1970 *Dynamic Hydrology*, McGraw-Hill, Inc, New York
[12] Byron F W and Fuller R W 1975 *Mathematics of Classical and Quantum Physics*, Vol. I, PWN, Warsaw (Polish edition)
[13] Patankar S V 1980 *Numerical Head Transfer and Fluid Flow*, Hemisphere Publishing Corporation, McGraw-Hill, Washington
[14] Le Veque R J 2002 *Finite Volume Methods for Hyperbolic Problems*, Cambrige University Press